Deformation, Damage and Fracture Behaviours of TWIP Steels Based on CZM-CPFEM at High Temperature

Wang Cai[1,2,4], Chaoyang Sun[1,2(✉)], Hongjia Zhang[3], Chunhui Wang[1,2], and M. W. Fu[4(✉)]

[1] School of Mechanical Engineering, University of Science and Technology Beijing, Beijing 100083, China
suncy@ustb.edu.cn

[2] Beijing Key Laboratory of Lightweight Metal Forming, Beijing 100083, China

[3] Vibration and Acoustics Research Group, Laboratory of Science and Technology On Integrated Logistics Support, College of Intelligence Science and Technology, National University of Defense Technology, Changsha 410073, China

[4] Department of Mechanical Engineering, Research Institute for Advanced Manufacturing, The Hong Kong Polytechnic University, Hung Hom, Kowloon, Hong Kong, China
mmmwfu@polyu.edu.hk

Abstract. Grain boundaries (GBs) are the most vulnerable areas of metals during high temperature forming and processing where microcracks are highly likely to affect their macroscopic properties, resulting in fracture and ultimately reduced service life. In order to investigate the mechanisms of micro- and nano-scale damage evolution, microcrack initiation and propagation, GBs must be included as a crucial consideration in the theoretical and modelling solutions. Thus, to accurately illustrate the influence mechanisms of GBs on the mechanical behaviours, the cohesive zone model (CZM) considering GB damage evolution and the crystal plasticity finite element model (CPFEM) coupling slip and twinning inside the grain, were combined to propose a micromechanical mechanism of TWIP steels, which is applicable to predict the strengthening, damage and fracture of TWIP steels under high temperature. The CZM-CPFE method was confirmed by in situ SEM experiments at 750 °C. The representative volume elements (RVEs) are constructed to predict the high temperature deformation behaviour of TWIP steels with different grain sizes and initial microdefects to obtain the influence of different initial states on the high temperature deformation behaviour, which can provide the solid theoretical basis for the subsequent manufacturing and forming processes of TWIP steel sheets. This work not only fills the gap in theoretical modelling of TWIP steels in the field of hot processing and manufacturing, but also provides some research approaches and analysis strategies for the GB damage behaviour of polycrystalline materials at high temperatures.

Keywords: TWIP steels · CZM-CPFEM · Grain boundary · High temperature · Damage and fracture

K. Mocellin et al. (Eds.): ICTP 2023, LNME, pp. 447–455, 2024.
https://doi.org/10.1007/978-3-031-41341-4_46

1 Introduction

The perfect combination of high uniform ultimate strength (>1 GPa) and considerable ductility (>60%) makes twinning-induced plasticity (TWIP) steels one of the most promising materials for the new generation of high strength steels for automotive applications [1]. The excellent mechanical properties of TWIP steels are due to the abundance of deformation twins and dislocation slips within the grain, and the synergy of the two mechanisms allows TWIP steels to maintain considerable toughness while increasing strength [2], which directly affects the manufacture of TWIP steel automotive components [3]. Therefore, the exploration of the microscopic mechanisms of plastic deformation can directly determine the prospects of TWIP steels in automotive and aerospace applications.

Grain boundaries (GBs) are a crucial factor of microcracks during the forming of polycrystalline materials, especially during high temperature forming and micro- and nano-scale processing [4]. Deformation, damage and fracture of GBs may directly lead to plasticity enhancement, microcracks initiation and propagation, which macroscopically affects their mechanical properties and eventually results in fracture and reduced service life [4]. Therefore, considering the damage evolution and fracture mechanism of GBs is vital for a more detailed understanding of the mechanical properties of TWIP steels under high temperature conditions for strength assessment and guidance of the forming process of components.

In this work, the cohesive zone model (CZM) [5] was used to describe the GB strengthening and damage evolution, the crystal plasticity with coupled slip and twinning to describe the grain interior deformation behaviours [6], the hardening law and flow rule considering temperature effect were introduced [7], the CZM-CPFE method was proposed, which was validated by in-situ SEM experiments at 750 °C. Based on CZM-CPFE method, the intergranular damage and failure behaviours of TWIP steel at high temperatures were investigated to reveal the influence law of factors such as grain size, GB angle and initial defects on damage and failure.

2 Methodology and Modeling

2.1 CZM-CPFE Method Considering Temperature Effect

Crystal plasticity is widely accepted to be one of the most effective tools for exploring microstructural damage and failure in metallic alloys [4–6]. To illustrate the interaction between grain interior and GBs, the CZM-CPFE method was developed based on prior work [7]. The deformation gradient tensor $\mathbf{F}$ is given by the following:

$$\mathbf{F} = \mathbf{F}^e\mathbf{F}^p = \mathbf{F}^e\mathbf{F}^{twin}\mathbf{F}^{slip} \tag{1}$$

The velocity gradient tensor $\mathbf{L}$ can be expressed by the following:

$$\mathbf{L} = \dot{\mathbf{F}} \cdot \mathbf{F}^{-1} = \dot{\mathbf{F}}^e \cdot \mathbf{F}^{e^{-1}} + \mathbf{F}^e \cdot \dot{\mathbf{F}}^p \cdot \mathbf{F}^{p^{-1}} \cdot \mathbf{F}^{e^{-1}} = \mathbf{L}^e + \mathbf{L}^p \tag{2}$$

where the plastic deformation velocity gradient tensor $\mathbf{L}^p$ benefits mainly from the contribution of slip and twinning, which is identified as the following:

$$\mathbf{L}^p = (1 - f_t^\beta) \sum \dot{\gamma}_T^\alpha \left(\mathbf{m}^\alpha \otimes \mathbf{n}^\alpha\right) + \sum \dot{\gamma}_T^\beta \left(\mathbf{m}^\beta \otimes \mathbf{n}^\beta\right) \tag{3}$$

where $f_t^\beta = \sum f^\beta$ is the sum of the twin volume fraction of all twin systems. Considering temperature effects, the slip shear rate $\dot{\gamma}_T^\alpha$ can be expressed as follows:

$$\dot{\gamma}_T^\alpha = \dot{\gamma}_0^\alpha \left| \frac{\tau^\alpha}{s^\alpha} \right|^{1/m} \operatorname{sign}(\tau^\alpha) \cdot \exp(-k\theta) \tag{4}$$

where $\dot{\gamma}_0^\alpha$ is the reference slip shear rate, τ^α is the resolved shear stress of the α slip system, s^α is the slip resistance, and m is the rate sensitivity factor [6], k is the thermal softening parameter [8], θ is a parameter related to temperature, which can be expressed by $\theta = \ln T_m - \ln(T_m - T)$. Similarly, the twin shear rate $\dot{\gamma}_T^\beta$ can be expressed as

$$\dot{\gamma}_T^\beta = \dot{\gamma}_0^\beta \left| \frac{\tau^\beta}{s^\beta} \right|^{1/n} \cdot \exp(-k\theta),\ \tau^\beta > 0;\ \dot{\gamma}_T^\beta = 0,\ \tau^\beta \le 0 \tag{5}$$

where $\dot{\gamma}_0^\beta$ is the reference twin shear rate, τ^β is the resolved shear stress on β twin system, s^β is the twin resistance, n is and rate sensitivity factor, and $m = n$ in the numerical calculation.

In addition, for GBs, based on prior work [7], the bilinear traction separation law for damage initiation is determined by the quadratic stress criterion (QUADS) and the damage evolution is determined by the power law, where the QUADS is given by the following:

$$f = \left\{ \frac{\langle \tau_n \rangle}{\tau_n^c} \right\}^2 + \left\{ \frac{\tau_s}{\tau_s^c} \right\}^2 + \left\{ \frac{\tau_t}{\tau_t^c} \right\}^2 \tag{6}$$

where τ_n, τ_s and τ_t denote stresses in the normal and two tangential directions. τ_n^c, τ_s^c and τ_t^c are the normal and two tangential damage initiation stresses. If $f = 1$, the GBs will immediately enter the damage stage. The power law can describe the damage evolution, which is defined by the following [5]:

$$\left\{ \frac{G_n}{G_n^C} \right\}^\lambda + \left\{ \frac{G_s}{G_s^C} \right\}^\lambda + \left\{ \frac{G_t}{G_t^C} \right\}^\lambda = 1 \tag{7}$$

where the power law exponent λ needs to be specified because the power law controls the fracture under mixed–mode loading. G_n, G_s and G_t denote the strain energy. G_n^C, G_s^C and G_t^C are the fracture toughness of the GBs. The QUADS and the power law are widely utilized to model damage and failure of composite materials. Practically, GBs are similar in geometry and mechanical characteristics to the bonding layers of composite materials. Therefore, the CZM constitutive relationship of the bilinear traction separation law is used to describe the damage and failure of GBs in this work.

2.2 Modeling and Parameters Calibration

The finite element modeling implementation based on CZM-CPFE method taking into account temperature effect is shown in Fig. 1. The CZM with GBs (Fig. 1(a)) and crystal plasticity with coupled slip and twinning (Fig. 1(b)) were established, respectively. Then, the open source software Neper was used to structure several RVEs with different grain sizes involving GBs [9]. The 4-node linear tetrahedron (C3D4) was utilized for the grains interior and the 6-node three-dimensional cohesive element (COH3D6) was considered for the GBs. These crystal plasticity constitutive relations are then written into the UMAT (user-defined materials subroutine) and given the material properties of the RVEs.

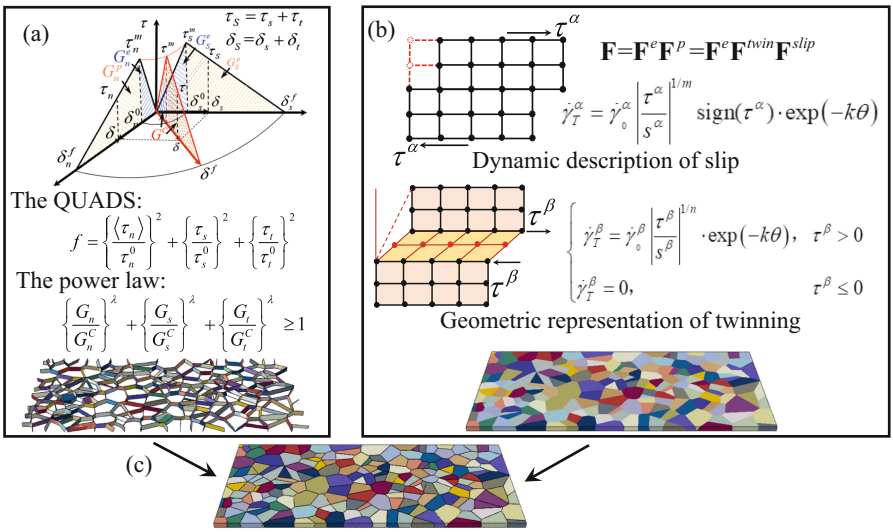

Fig. 1. The finite element modeling implementation based on CZM-CPFE method: (a) grain boundary constitutive equations of CZM and (b) crystal plasticity of grain interior. (c) RVE of strengthening, damage and fracture of TWIP steels considering temperature effect.

The parameters of the grain boundary CZM in Fig. 1(a) are shown in Table 1. K_{nn}, K_{ss} and K_{tt} denote the normal and two tangential stiffness of the GBs, respectively. σ_s is the experimentally measured yield stress, and T_{n}, T_{s} and T_{t} are the thicknesses in the calculations and set to a constant of 1. Furthermore, the parameters of crystal plasticity within grains are selected as shown in Table 2, where C_{11}, C_{12} and C_{44} are elastic constants, ν is the Poisson's ratio, the critical value of f_t^{β}, f_0, is 0.4 and the melting point temperature $T_m = 1500$ °C of the TWIP steel is selected.

Table 1. Constitutive parameters of CZM considering GBs.

K_{nn} (GPa)	K_{ss}, K_{tt} (GPa)	τ_n^c (MPa)	τ_s^c, τ_t^c (MPa)	λ	T_n, T_s, T_t
210	84	1.2 σ_s	0.4 τ_n^c	1	1

Table 2. Constitutive parameters of crystal plasticity at 750 °C.

C_{11} (GPa)	C_{12} (GPa)	C_{44} (GPa)	ν	$\dot{\gamma}_0$ (s^{-1})	k
198	125	122	0.25	0.001	5
s_0^α (MPa)	s_0^β (MPa)	f_0	m	n	T_m (°C)
75.3	101	0.4	0.02	0.02	1500

3 Experiments and Model Validation

3.1 Experiments and Characterization

The typical Fe-Mn-Si-Al TWIP steel was wire-cut electrical discharge machining into in-situ tensile specimens with a 2 × 1 mm^2 (length × width) gauge area, which are ground, polished and eroded until clear grain morphology can be observed. The prepared specimens are clamped in an in-situ tension device with a heater and placed in an SEM (TESCAN S8000) [7]. The specimen is heated to the target temperature (750 °C) and loaded at a constant strain rate of 7.5 × 10^{-5} s^{-1}. The macroscopic mechanical data is output and the relevant microstructural features are captured using the SEM.

In addition, in order to determine the orientation and size of the RVE sets, the specimens were subjected to EBSD (electron backscattered diffraction) characterisation to obtain the grain orientation and size. The RVE grain orientation is then assigned by writing the code into UMAT and the dimensions of the RVE are set to 0.2 × 0.1 × 0.02 mm^3. The EBSD data was analysed by the HKL channel 5 software package based on the TSL-EDAX EBSD system [10].

3.2 Validation of RVE

Based on the ABAQUS software platform, the RVE was uniaxially loaded after setting the boundary conditions to output the corresponding stress-strain curves for comparison with the in-situ tensile experiments at 750 °C. The results are shown in Fig. 2. It can be seen that the CZM-CPFE method can well simulate the macroscopic mechanical behaviours and the experimental and simulated stress-strain curves agree well at high temperature. Moreover, the stress concentration near the GBs is verified by the areas marked by the red solid circles in Fig. 2. Meanwhile, the experimental and simulated ultimate tensile strength and failure strain values are very close. Thus, the accuracy and reliability of CZM-CPFE method is confirmed by the experimental mechanical properties and microstructural evolution.

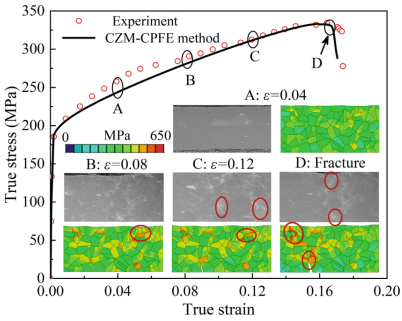

Fig. 2. Comparison of experiments and RVE simulations based on the CZM-CPFE method, where the microstructural evolution is highlighted of A: $\varepsilon = 0.04$, B: $\varepsilon = 0.08$, C: $\varepsilon = 0.12$ and D: fracture. The red solid circles indicate the areas of stress concentration.

4 Discussion and Analysis

4.1 Effect of Grain Size

The influence of grain size on mechanical properties is well known, and for metallic materials, the effect of grain size on forming and fabrication processes is significant, mainly due to the correlation between yield stress and GBs damage by grain size [7]. Therefore, in order to exploit the application of the CZM-CPFE method for damage and failure prediction in the forming and manufacturing process of polycrystalline materials, models with different grain sizes were developed. By comparing the stress-strain curves in Fig. 3(a), it can be noted that the failure strain increases as the grain size decreases, and the yield strength and ultimate tensile strength also increase, which may be related to the densification of the GBs. Thus, the scalar stiffness degradation (SDEG) and strain energy curves of the GBs are obtained as depicted in Fig. 3(b) and (c), it is seen that the increase in the number of GBs can delay fracture, which results in the GBs to store more strain energy.

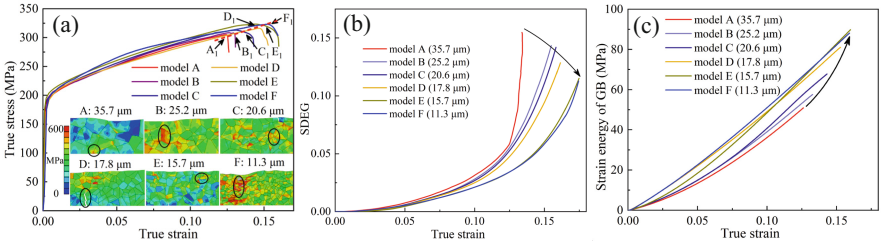

Fig. 3. Mechanical properties of TWIP steels with different grain sizes at 750 °C: (a) stress-strain curves and microstructural evolution; (b) the SDEG and (c) strain energy stored during GBs deformation, damage and fracture.

4.2 Effect of GB Angle

The misorientation difference of neighbouring grains, i.e. the GB angle, plays a crucial role in microfabrication mechanics [9]. In order to explore the effect of the GB angle on the damage and failure, the RVE of the neighbouring grains based on the prior work [7] was established by giving different orientations to the two grains to achieve different GB angles, and simulation results of RVEs with different GB angles in the range of 10 to 70° were obtained. As shown in Fig. 4(a), it can be seen that the failure strain decreases as the GB angle increases, which may be directly related to the grain boundary energy [7]. Simultaneously, the GB strength is higher than that of the grain interior, and the quadratic stress damage initiation criterion (QUADSCRT) and SDEG of the GB damage increase rapidly with increasing GB angle, especially near the 60° grain boundary, where the value of SDEG rapidly increases to near 1. As shown in Fig. 4(b), the strain energy of GB is closely related to the GB angle, and low angle grain boundaries appear to be able to store more strain energy to facilitate coordinated deformation. On the other hand, high angle grain boundaries appear to be fragile and are not conducive to coordinated deformation, which in turn leads to rapid fracture.

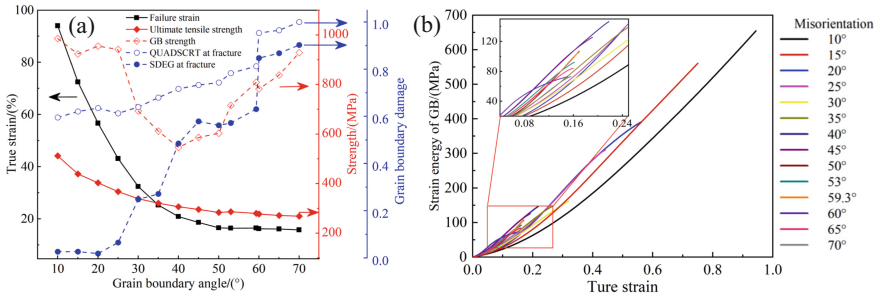

Fig. 4. (a) Strength, failure strain, damage and (b) stored strain energy of GB angles between 10 and 70°.

4.3 Effect of Initial Void Defect

The presence of some initial microvoids introduces significant uncertainty into the prediction of microcracking behaviour during machining, forming and fabrication [7]. Therefore, four different locations and five different sizes of microvoid models were developed and the simulation results are shown in Fig. 5. The Y highlight in Fig. 5(a) shows that the location of the microvoids affects the yield strength of the material. Defects at the edges reduce the yield strength and uniform tensile strength. Furthermore, internal microvoids seem to be more likely to cause damage and the stored strain energy at GBs is reduced in Fig. 5(b) and (c).

The results in Figs. 5(d) to (f) show that the yield strength (M marked), the uniform tensile strength and the uniform elongation also decrease with microvoid size increasing, the GBs are more prone to damage and the stored strain energy of the GBs also decreases.

These results provide a good indication for the application of the CZM-CPFE method to the processing and manufacturing and can also provide some reference for specifying relevant processing.

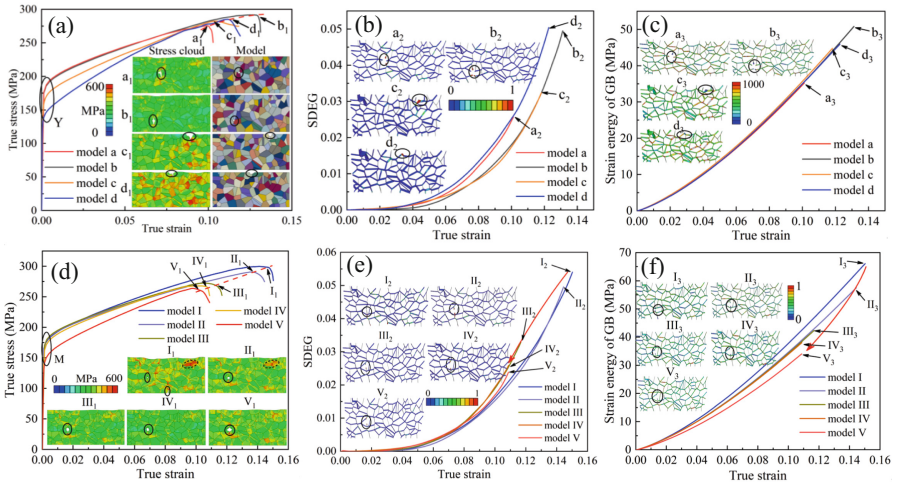

Fig. 5. Location and size of initial microvoids: (a) (d) the stress-strain curves, (b) (e) the SDEG distribution and evolution and (c) (f) the stored strain energy of GBs. Black solid circles indicate the initiation of fracture microcrack.

5 Conclusion

A CZM-CPFE method considering temperature effects that can predict intergranular cracking was developed and its validity and accuracy were confirmed by in-situ tensile experiments at 750 °C. The RVEs based on CZM-CPFE method analysed the effects of grain size, GB angle and initial microvoid defects on the damage and failure of TWIP steels, obtaining that smaller grain sizes, lower angle grain boundaries and smaller microvoid sizes are more resistant to damage and more beneficial to the forming and fabrication of components.

Acknowledgements. The authors acknowledge the funding supported by the National Natural Science Foundation of China (No. 52175285, 52161145407, U22A20186, 52001325). Wang Cai would like to thank the project of G-SB4Y from the Hong Kong Polytechnic University (PolyU) of the Joint Supervision Scheme for his PhD study in PolyU.

References

1. De Cooman, B.C., Estrin, Y., Kim, S.K.: Twinning-induced plasticity (TWIP) steels. Acta Mater. **142**, 283–362 (2018)

2. Kim, J.K., Kwon, M.H., De Cooman, B.C.: On the deformation twinning mechanisms in twinning-induced plasticity steel. Acta Mater. **141**, 444–455 (2017)
3. De Cooman, B.C.: High Mn TWIP Steel and Medium Mn Steel, Automotive Steels, pp. 317–385. Woodhead Publishing, Sawston (2017)
4. Li, H., Huang, D., Zhan, M., Li, Y., Wang, X., Chen, S.: High-temperature behaviors of grain boundary in titanium alloy: modeling and application to microcrack prediction. Comput. Mater. Sci. **140**, 159–170 (2017)
5. Alabort, E., Barba, D., Sulzer, S., Lißner, M., Petrinic, N., Reed, R.C.: Grain boundary properties of a nickel-based superalloy: characterisation and modelling. Acta Mater. **151**, 377–394 (2018)
6. Sun, C.Y., Guo, N., Fu, M.W., Wang, S.W.: Modeling of slip, twinning and transformation induced plastic deformation for TWIP steel based on crystal plasticity. Int. J. Plast **76**, 186–212 (2016)
7. Cai, W., Sun, C., Wang, C., Qian, L., Li, Y., Fu, M.W.: Modelling of the intergranular fracture of TWIP steels working at high temperature by using CZM–CPFE method. Int. J. Plast **156**, 103366 (2022)
8. Liu, X., Sun, W.K., Liew, K.M.: Multiscale modeling of crystal plastic deformation of polycrystalline titanium at high temperatures. Comput. Methods Appl. Mech. Eng. **340**, 932–955 (2018)
9. Quey, R., Dawson, P.R., Barbe, F.: Large-scale 3D random polycrystals for the finite element method: Generation, meshing and remeshing. Comput. Methods Appl. Mech. Eng. **200**(17–20), 1729–1745 (2011)
10. Cai, W., Wang, C., Sun, C., Qian, L., Fu, M.W.: Microstructure evolution and fracture behaviour of TWIP steel under dynamic loading. Mater. Sci. Eng. A **851**, 143657 (2022)